

KARMA



Karst Aquifer Resources availability and quality in the Mediterranean Area

Application of Artificial Neural Network models at KARMA test sites
Deliverable 4.3

Authors:

Andreas Wunsch (KIT), Tanja Liesch (KIT), Nico Goldscheider (KIT), Emna Gargouri-Ellouze (ENIT), Tegawende Arnaud Ouedraogo (ENIT), Fairouz Slama (ENIT), Rachida Bouhlila (ENIT), Guillaume Cinkus (UM), Naomi Mazzilli (UM), Hervé Jourde (UM)

Date: August 2021



This project has received funding from the European Union's PRIMA research and innovation programme



Project Partners



(Coordinator)



SAPIENZA
UNIVERSITÀ DI ROMA



Participant No *	Organization	Country
1 (Coordinator)	Karlsruhe Institute of Technology (KIT)	Germany
2 Partner 1	Federal Institute for Geosciences and Natural Resources (BGR)	Germany
3 Partner 2	University of Malaga (UMA)	Spain
4 Partner 3	University of Montpellier (UM)	France
5 Partner 4	University of Rome (URO)	Italy
6 Partner 5	American University of Beirut (AUB)	Lebanon
7 Partner 6	Ecole Nationale d'Ingénieurs de Tunis (ENIT)	Tunisia

Executive Summary

Work package 4 of the KARMA project focuses on the development and comparison of transferable modelling tools for improved predictions concerning the impacts of climate change, floods, droughts and land-use changes on karst aquifers. In this context, the application of Artificial Neural Networks to model karst spring discharge time series is demonstrated in deliverable 4.3. Modeling results from six different test sites are shown by using an approach based on 1D-Convolutional Neural Networks, which have been shown to be fast and reliable for strongly related tasks such as groundwater level predictions. Using this approach, even for complex systems, highly accurate results can be achieved with comparably little time effort and only little prior knowledge about the system being necessary. However, no deeper knowledge of the system can be derived from the model and in areas where too few data are available, no satisfying results can be achieved.

Accompanying model codes will be published as part of deliverable 4.4.

1 Table of Content

Technical References	2
Version History	2
Project Partners	3
Executive Summary.....	4
2 Introduction	6
3 Material and Methods.....	7
3.1 Available Data	7
3.2 Available Data and Preprocessing - Zaghouan Site	8
3.3 Convolutional Neural Networks	11
3.4 Model Calibration and Evaluation	11
3.5 Alternative Approach – Zaghouan Site	12
3.5.1 ANN Models	12
3.5.2 Simulation and Evaluation Approach.....	13
4 Results and Discussion	14
4.1 Aubach Spring (Austria)	14
4.2 Lez Spring (France)	15
4.3 Unica Springs (Slovenia).....	15
4.4 Gato Cave Spring (Spain).....	16
4.5 Qachqouch Spring (Lebanon)	17
4.6 Nymphaea Spring (Tunisia)	18
4.6.1 MLP	18
4.6.2 CNN	19
4.6.3 LSTM.....	20
4.7 Comparison with lumped parameter model results	21
5 Conclusions.....	22
References.....	22

2 Introduction

Modeling Karst water resources is challenging, because water flow is highly variable due to the unknown conduit networks. Therefore a large variety of different modeling approaches exists (Jeannin et al., 2021), most of them requiring a certain level of background knowledge about the system in order to achieve high quality results. In contrary, deep learning approaches can be applied without detailed system knowledge necessary, by being able to establish a relationship between relevant forcings, such as climatic inputs, and outputs, i.e. spring discharge, on their own. To date, Artificial Neural Networks (ANN) remain an exotic tool in the karst modeling community. Nevertheless, different types of ANNs have been applied in modeling karst water resources for quite a long time, with the study of Johannet et al. (1994) being even one of the first applications of ANNs in water related research. In the context of the KARMA project mainly Convolutional Neural Networks (CNN) are applied to model karst spring discharge at several sites. CNNs have been shown to be fast and reliable for the closely related application of groundwater level forecasting (Wunsch et al., 2021) and also have been rudimentarily applied to Karst spring modeling (Jeannin et al. 2021). According to the study of Wunsch et al. (2021), CNNs are significantly faster and more stable than other methods such as NARX (nonlinear autoregressive models with exogenous inputs) and LSTM (long short-term memory networks), and usually show similar or better accuracy in predicting groundwater levels, which makes them the preferable approach for modeling karst spring discharge. Even though such data driven approaches rely on a comparably large data basis and do usually not enhance system knowledge such as lumped parameter models can do, they are a powerful tool to achieve high quality simulations in a relatively short time.

All KARMA test sites were scanned for a suitable data basis to apply ANN modeling. Because of the fact that gapless and as long as possible time series of both spring discharge (target variable) and climatic inputs (i.e. precipitation, temperature, etc.) have to be available, the Eastern Ronda Mountains test site in Spain and the Gran Sasso test site in Italy were not suitable for ANN application. A large number of data gaps and too short time series prevented ANN application in these two areas. The Zaghouan site in Tunisia holds a somewhat unique position in this respect. On the one hand, the data are very old and had to be digitized first, on the other hand, a certain effort was made to generate input data and thus build models, while the other sites were modeled with current and already existing meteorological series. The modeling here was done exclusively by the local partner ENIT and therefore includes some further analysis and a brief comparison of CNNs with two other types of models, namely Multi-Layer Perceptron (MLP) and Long Short-term Memory (LSTM) models. For these reasons the Zaghouan site is presented in separate sub topics in this report.

To compensate for the two unusable test sites in Spain and Italy, additional alternative karst areas/springs were used for ANN modeling, so that results from a total of six karst springs can be presented: Aubach spring (Hochifen-Gottesacker karst area) in Austria, Lez spring in France, Unica springs in Slovenia, Gato cave spring in Spain, Qachqouch spring in Lebanon and Nymphaea spring (Zaghouan area) in Tunisia (Figure 1). For descriptions of the study areas we refer to Deliverable 4.2. In this report we will focus on description of data, models and results.

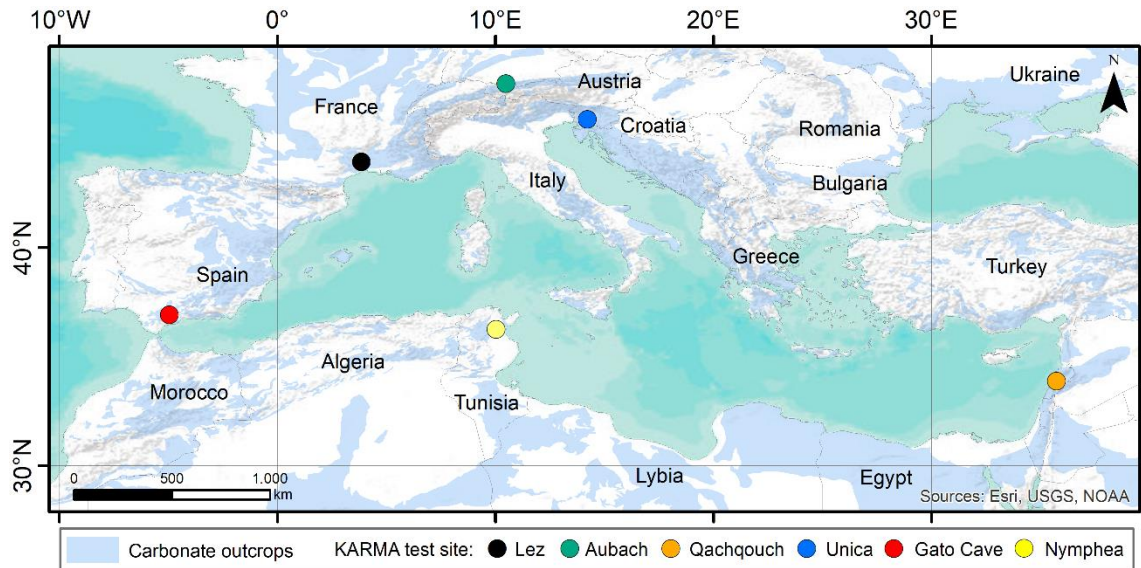


Figure 1: Location of the karst springs modeled with ANNs and carbonate outcrops after WOKAM (Chen et al., 2017a)

3 Material and Methods

3.1 Available Data

Very different data were available for each site especially in terms of climatic parameters, temporal resolution and available period. Table 1 gives a summary of the used data for each site. Sometimes more parameters, additional climate stations, other periods or even other temporal resolutions were available and have been tested. The used data represents a compromise of longest available time period, as large as possible number of relevant parameters, and model performance.

Table 1: Data basis overview of all five modeled sites.

Spring	Period	Temporal Resolution	Input Parameters
Aubach	2012-2020	Hourly	Precipitation, temperature and snow routine output for climate stations Walmendinger Horn, Diedamskopf and Oberstdorf. Additional Parameter: Tsin
Lez	2008-2019	Daily	Precipitation (interpolated), Prades-le-Lez climate station: temperature
Unica	1961-2018	Daily	Postojna climate station: precipitation, pot. evaporation, temperature, rel. humidity, snow, new snow; Cerknica climate station: precipitation, snow, new snow
Gato Cave	1970-2015	Daily	Precipitation, temperature
Qachqouch	2015-2020	Daily	Climate station 1 (950m): temperature, rel. humidity; climate station 2 (1750m): temperature, precipitation, evapotranspiration

In case of Aubach spring the discharge is significantly influenced by seasonal snow accumulation and melting (Chen et al., 2017b) and no directly measured data about snowfall or snowmelt were available. Therefore a snowmelt routine is run as preprocessing of the meteorological input data as described in

Application of Artificial Neural Network models

Chen et al. (2018). This routine is a slightly modified version (after Hock 1999) of the HBV hydrological model snow routine (e.g. Bergström 1975, 1995; Seibert 2000; Kollat et al. 2012), which redistributes the precipitation time series in accordance with probable snow accumulation and snowmelt and produces an additional input parameter for each climate station. Such parameter can potentially replace the original precipitation input; however, the performance of the model was better when including both the original and the redistributed precipitation. Other test sites either had snow data from climate stations available (e.g. Unica) or are not (significantly) influenced by snow accumulation and snowmelt (e.g. Lez). This is also shown in Deliverable 4.2, where a precipitation redistribution using this snow routine for all sites is performed and significant redistribution can be observed only for Aubach and Unica.

In some cases, ANN models can profit from artificial input data that provides information on the season and therefore the current position in the annual cycle. Therefore, the influence of a sinus signal input fitted to the temperature curve (Tsin), which is known from experience to often improve modeling results, is tested. For one of the five sites (Aubach spring) such input provided improved performance and was therefore also used.

3.2 Available Data and Preprocessing - Zaghouan Site

In our ANN modelling approach, the data used are: the meteorological input data or exogenous data to the karst and the output data (discharge) or endogenous data. The input data considered are rainfall, mean temperature and pressure on a daily scale. The rainfall data considered are those of the "Zaghouan controle" station (latitude: 36.39583; longitude: 10.14917) which extend from 1915 to 1944. However, there are gaps in the data for the entire year of 1929 and January 1930. These gaps were filled by a linear interpolation using data from the nearby station "Zaghouan SM" (latitude: 36.40306; longitude: 10.14472) (Figure 2).



Figure 2: Location of study rainfall stations

This data treatment allows us to obtain the entire series of daily and weekly cumulative rainfall (Figure 3 and Figure 4).

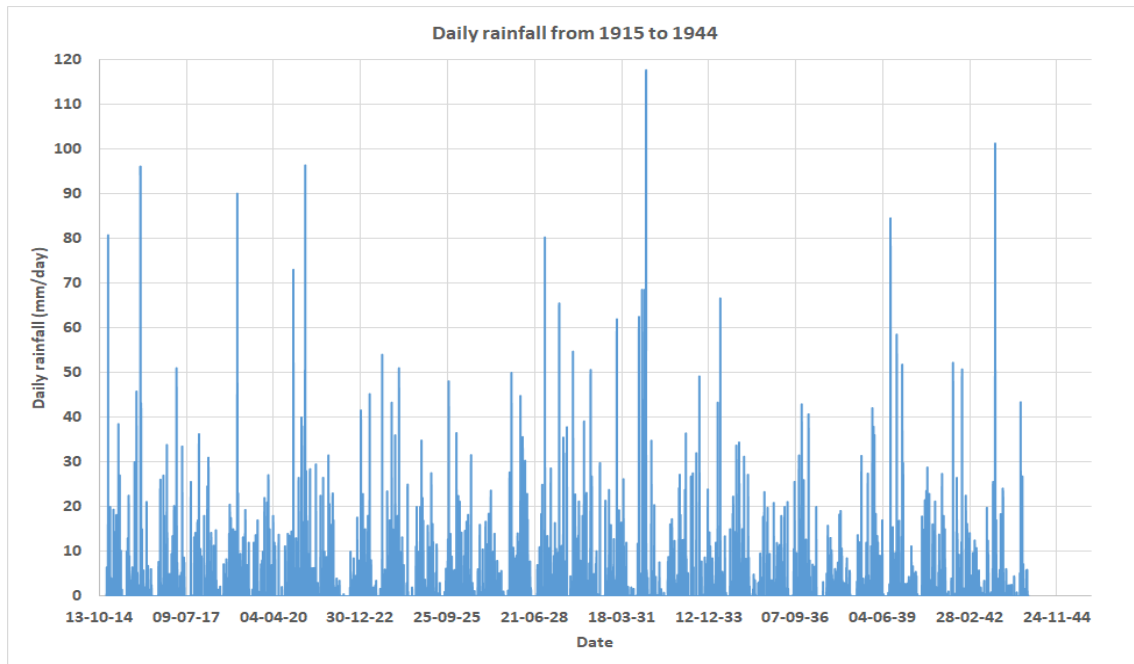


Figure 3: Daily rainfall from 1915 to 1944 at Zaghuan contrôle station

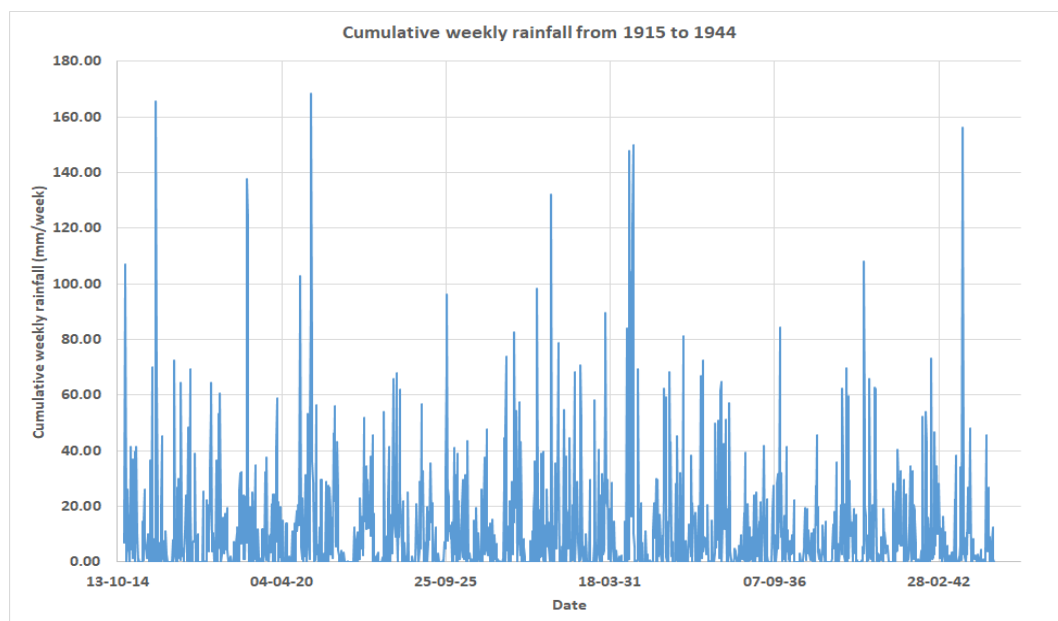


Figure 4: Cumulative weekly rainfall from 1915 to 1944 at Zaghuan contrôle station

A statistical description of the weekly rainfall series gives us the following table (Table 2). It can be seen that the first quartile for weekly series is equal to 0 mm, which is explained by the low number of rainy days, 77 days per year (this is most noticeable for the daily series). Indeed, Zaghuan is located in a semi-arid zone. In addition to the rainfall data used as input, we used a synthetic daily and weekly series of median temperature and pressure values, as data from 1915 to 1943 are not available at the moment. This synthetic series was built up from temperature and pressure data from 1943 to 2008 from the Oued El Kebir dam. Figure 5 shows the different percentiles on a weekly and daily scale. Subsequently, we considered the median and repeated it several times to obtain our weekly and daily temperature and pressure series.

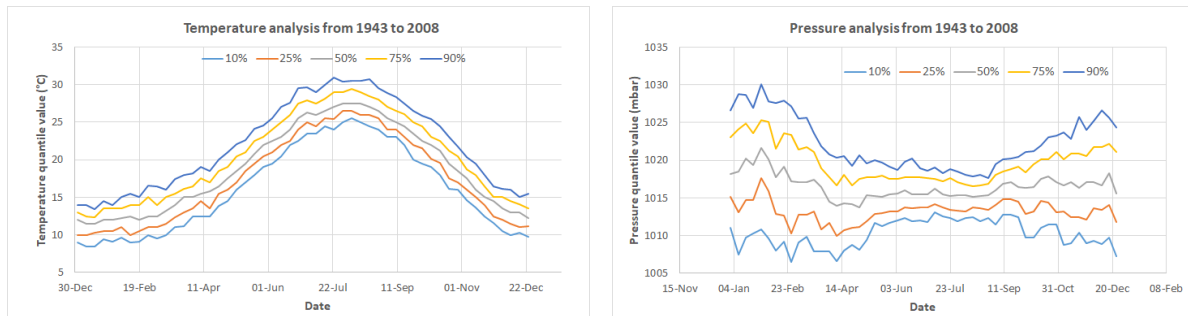


Figure 5: Synthetic temperature (left) and pressure (right) series from 1943 to 2008

The discharge series at the source of the Nymphaea is the output. The discharge is the result of the hydrodynamic transformation of the input data by the karst, in our case the rainfall. Since we only have discharge series in graphical form from 1915 to 1944 at irregular time scales, our first task has been to digitize these discharge data. This digitalization allowed us to obtain a complete, continuous, and regular discharge series on a weekly scale (fig 7). The discharge on a daily scale were obtained by linear interpolation, as was done in the work of Sagna (2000) and Faydi (2021). As with our climatic series, we considered statistical analysis and understanding before modelling. As a result, we obtain the following descriptive Table 2.

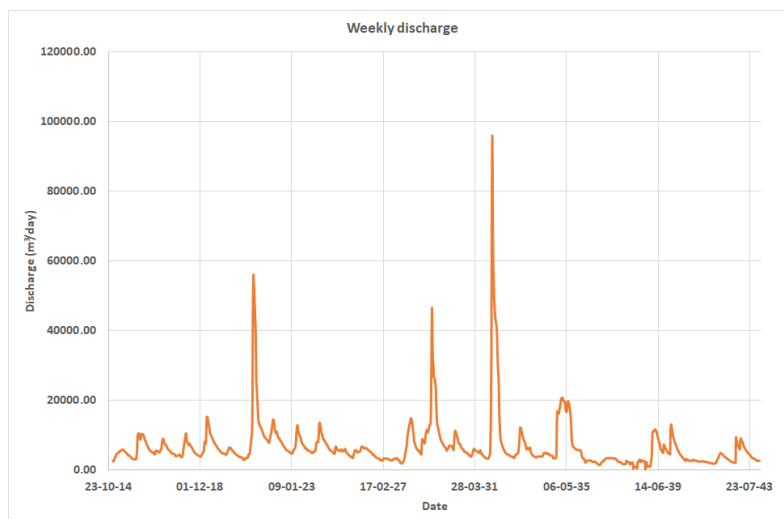


Figure 6: Weekly discharge from 1915 to 1944

Table 2: Statistical description of the rainfall (left) and discharge (right) time series.

Rainfall	Weekly	Daily	Discharge	Weekly	Daily
Number of rainfall values	1,514	10,592	Number of discharge values	1,514	10,592
Mean (mm)	11.7	1.4	Mean discharge (m ³ /day)	6,984	6,987
Standard deviation	20.1	5.5	Standard deviation (m ³ /day)	7,151	7,159
Min (mm)	0	0	Min discharge (m ³ /day)	216	216
25% quartile (mm)	0	0	25 % quartile (m ³ /day)	3,605	3,606.7
50% quartile (mm)	3.7	0	50 % quartile (m ³ /day)	5,337	5,350.3
75% quartile (mm)	14.3	0	75 % quartile (m ³ /day)	5,337	7,631.5
Max (mm)	168.4	117.3	Max discharge(m ³ /day)	98,530	98,530

3.3 Convolutional Neural Networks

Convolutional Neural Networks (LeCun et al., 2015) are a common tool in object recognition, image classification and signal processing. The general structure usually uses sequences of blocks, consisting of several layers, which are typically at least one convolutional layer and a pooling layer. The dimension of the data predefines the dimension of the convolutional layers (1D in case of time series) that use filters with a fixed size (kernel size, receptive field) to produce a certain number of feature maps of the input data. Often a larger number of filters is used, each of them recognizing different input data characteristics (features). Afterwards downsampling and therefore information consolidation is performed in a pooling layer. A wide range of model structures based on these blocks are possible. Usually additional layers to prevent, for example, exploding gradients (e.g. using batch normalization layers) or overfitting of the model (e.g. using dropout layers) are also used within such block sequences. Often long short-term memory networks are preferred over 1D-CNNs because they are by definition not prone to the vanishing gradient problem, nevertheless we have shown in earlier studies (Wunsch et al., 2021) that for groundwater modeling 1D-CNNs are superior because they are faster, often show higher performance and furthermore produce reliably stable results.

We use an ensemble of 10 models to reduce the dependency of the model on the random initialization of the layer weights and calculate 100 forecasts for each of these 10 models based on a Monte-Carlo dropout approach, which are used to derive the 95%-model uncertainty interval. Each of the used CNN models follows the general design shown in Figure 7. Hyperparameters are derived as described in the following section. Python 3.8 (van Rossum, 1995) and the following frameworks and libraries are used to implement all models: TensorFlow and its Keras API (Abadi et al., 2015; Chollet, 2015), Numpy (van der Walt et al., 2011), Pandas (McKinney, 2010; Reback et al., 2020), Scikit-Learn (Pedregosa et al., 2011), Unumpy (Lebigot, 2010), Matplotlib (Hunter, 2007) and Bayesian Optimization (Nogueira, 2014).

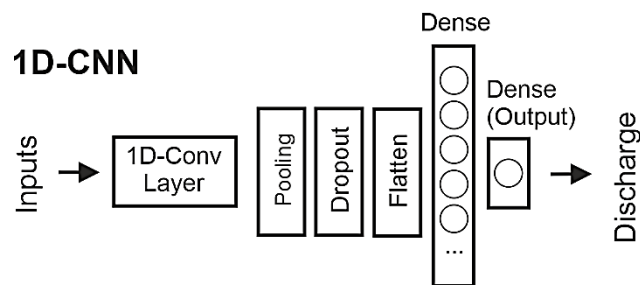


Figure 7: CNN model design used to simulate karst spring discharge

3.4 Model Calibration and Evaluation

While training, optimizing and testing the model, data leakage is prevented by splitting the time series of each site into four parts of which the largest part is used for training, a smaller part for early stopping to prevent overfitting the model (validation), and two other parts as test set during optimization and as final test set to evaluate the model performance (Table 3).

Table 3: Time series splitting for each test site for model training, optimization and testing

	Training	Validation	Optimization	Testing
Aubach	11/2012-2017	2018	2019	1/2020-10/2020
Lez	10/2008-2015	2016	2017	2018+2019
Unica	1961-08/2012	09/2012-10/2014	11/2014-09/2016	10/2016-2018
Gato Cave	1970-08/2003	09/2003-08/2007	09/2007-08/2011	09/2011-05/2015
Qachqouch	09/2015-09/2018	10/2018-02/2019	02/2019-09/2019	10/2019-01/2020

Further, Bayesian optimization is used to derive the length of the input sequence (search space is site dependent), the batch size (2^4 to 2^8) during training, the number of filters in the 1D-Conv layer (2^4 to 2^8), and the number of neurons in the first dense layer (2^4 to 2^8). These hyperparameters are optimized on model performance in terms of mean squared error (objective function) in the optimization set. While the kernel size was set to 3 for all of the models, the dropout rate was chosen site dependently (as high as possible with meaningful results, at least 10%), as well as the number of training epochs, the early stopping patience and the number of Bayesian optimization steps (Table 4). We mostly perform at least 50 optimization steps and stop either when 80 steps are reached or after no improvement for 10 steps (Stop Criteria).

Table 4: Manually chosen Hyperparameters.

	Dropout Rate	Training Epochs	Early Stopping Patience	Bayesian Optimization Steps (Min/Max/Stop Criteria)
Aubach	10%	200	20	50/80/10
Lez	50%	200	15	25/50/10
Unica	10%	100	10	50/80/10
Gato Cave	50%	100	10	50/80/10
Qachqouch	10%	500	20	50/80/10

To evaluate the performance of the models, several metrics are calculated: Nash-Sutcliffe Efficiency (NSE) (Nash and Sutcliffe, 1970), squared Pearson r (R^2), root mean squared error (RMSE), Bias (Bias) as well as Kling-Gupta-Efficiency (KGE) (Gupta et al., 2009). For squared Pearson r the notation of the coefficient of determination (R^2) is used, because the linear fit between simulated and observed discharge, thus of a simple linear model is compared, which makes them equal in this case. Further, individual performance on high, medium and low flow were investigated using mainly RMSE and Bias. Especially, NSE and KGE seem rather unintuitive for such evaluation, because the reference values for calculation change, which makes comparison and interpretation difficult. The thresholds to distinguish between high/medium and medium/low flow are defined as the 90% quantile of Q and 40% of the mean Q value, respectively.

3.5 Alternative Approach – Zaghuan Site

3.5.1 ANN Models

In a comparative modelling approach, we considered three types of ANN models: Multi-layer perceptron (MLP), Long Short-Term Memory (LSTM) and Convolutional Neural Network (CNN). In addition, in order to characterize the most suitable time scale for our system, we performed daily and weekly simulations for each model. For each temporal approach, a simulation configuration has been adopted: it consists in predicting a single future value of flow knowing only the data on rainfall, average temperature and pressure of the previous days. This configuration is called "seq2val forecasting" or "one-step ahead forecasting". In order to prevent overfitting, we used the "dropout" regularization method which consists in randomly deactivating some neurons at each iteration.

The MLP model is a model consisting of interconnected neurons. It has hidden layers of N_c neurons each and a linear output layer consisting of one neuron (Kong-A-Siou et al., 2015). Our MLP model consists of two hidden layer and one linear output neuron.

The LSTM model is a recurrent neural network model. It uses stochastic approximation through sequential time series. It consists of several cells; each cell comprising the input gate, the output gate and the forget gate. The LSTM model incorporates previous predictions into current predictions (Mbah et al., 2021). Our LSTM model consists of an LSTM layer that is connected by a linear output neuron.

Mostly used in image recognition and classification, convolutional neural networks find their use in the prediction of continuous signals such as source flows. The typical structure of a CNN is already described in Section 3.3.

3.5.2 Simulation and Evaluation Approach

The input data for our models are rainfall, temperature and pressure; the output data is the discharge at the source of the Nympea. Our modelling consists of two phases: a calibration/training phase and an evaluation phase. According to this distribution, we have split our data. Thus, 85% (24 years) of the data will be used in the calibration phase and 15% (4 years) of the data in the evaluation phase (Figure 8). Furthermore, in view of the nature of the activation functions and in order to guarantee a better distribution of the data and to facilitate predictions, we have standardized our data between 0 and 1. This operation has the merit of improving the performance of our models (Shanker et al., 1996).

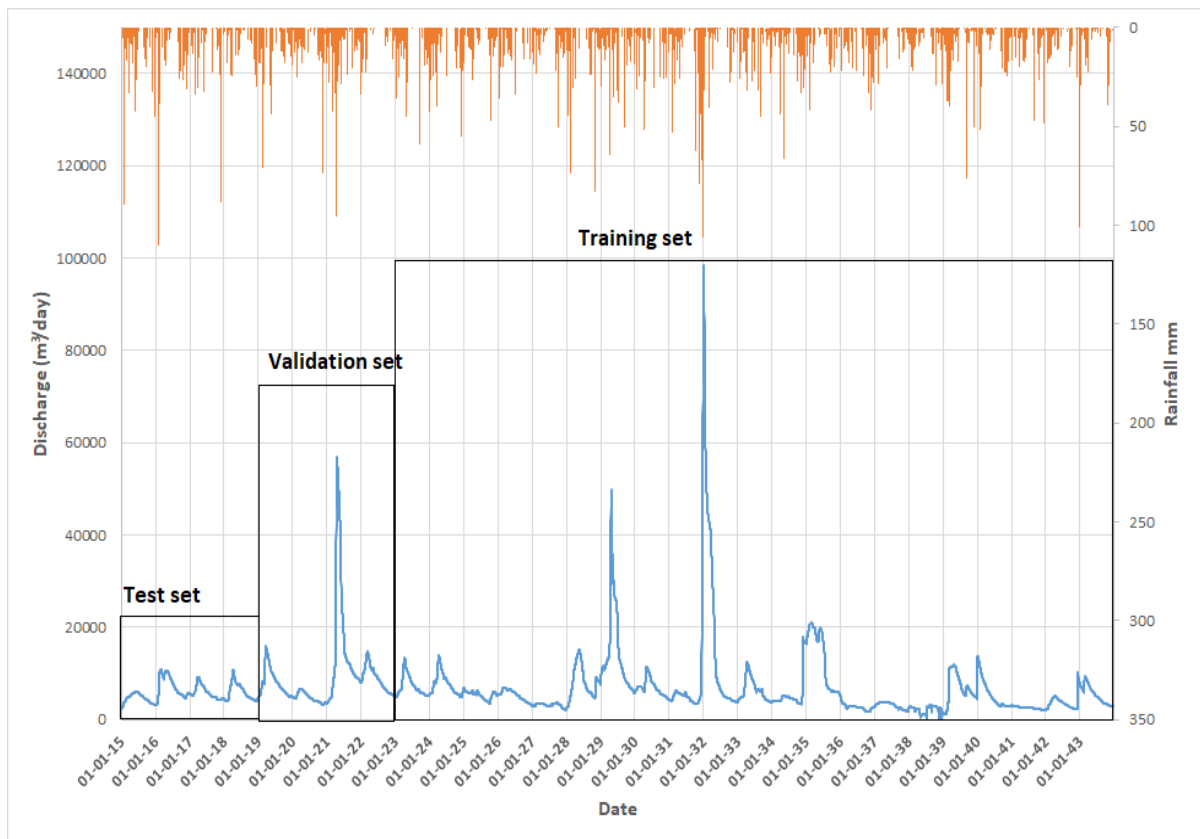


Figure 8: Data splitting at Zaghouan Site

Our different models have hyperparameters which are the guiding part of the simulations. However, it is not obvious to find the optimal combination of hyperparameters. Therefore, we used Bayesian optimization (Nogueira, 2014) to ensure optimal performance. We used the acquisition function "expected improvement" or (EI); the function to be maximized being: $f(x) = NSE + R^2$ (Wunsch et al., 2021).

The evaluation parameters of our models are: R^2 , NSE, Bias, RMSE, rRMSE, rBias. Through these parameters, we were able to compare our models and judge their predictive accuracy.

4 Results and Discussion

4.1 Aubach Spring (Austria)

The modeling results for the evaluation/test period (1/2020-10/2020) of the CNN model at Aubach spring are shown in Figure 9. The model was able to accurately model the spring discharge during most periods of the test section with high NSE (0.82) and KGE (0.90) values. The second highest peak of the whole time series occurs in February and is only slightly underestimated. The snowmelt-influenced period from April to Mid-June is accurately modeled as well as the peaks in summer and early autumn. In October, a series of peaks can be observed that is not well captured by the model output. A plausible explanation is that the input data does not capture the respective local precipitation events because of the location of the climate stations outside of the catchment.

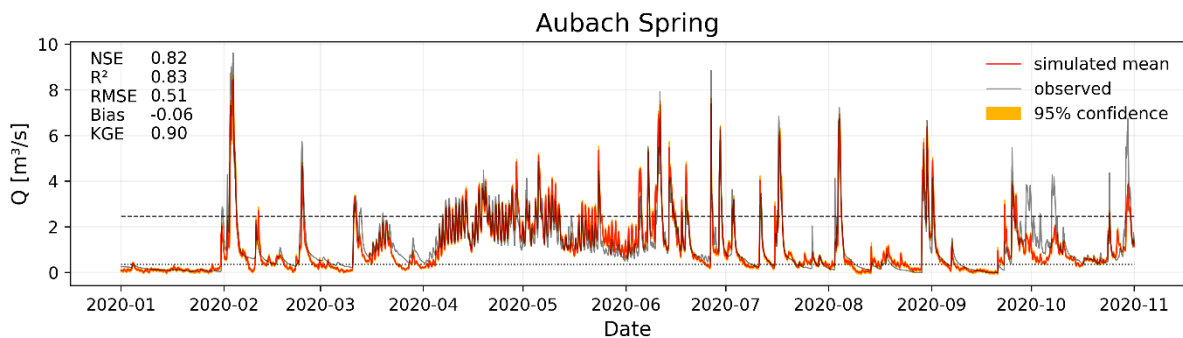


Figure 9: Modeling results for Aubach spring in 2020. Dashed and dotted lines: thresholds to determine low, medium and high flow.

Regarding the model performance for low, medium and high flow parts of the test period, RMSE and Bias are shown in Table 5. While high and medium flow are systematically underestimated, low flow is slightly overestimated. The RMSE is satisfying in general and as expected largest for the simulation of the high flow peaks.

Table 5: Low, medium and high flow evaluation of the model performance at Aubach spring.

	RMSE [m ³ /s]	Bias [m ³ /s]
Total	0.51	-0.06
High Flow	1.01	-0.33
Medium Flow	0.43	-0.04
Low Flow	0.22	0.03

The model uncertainty is very low, especially compared to the discharge variability. Aubach spring catchment, as part of the Hochiften-Gottesacker karst system is complex and challenging to model with conventional models such as lumped parameter models, due to high differences in altitude, and high precipitation heterogeneity (including snow accumulation influence). Despite these facts and sub-optimal climate station positioning outside the catchment, the CNN model is able to satisfyingly and accurately model the discharge time series. The relatively long time series with a very high temporal resolution (hourly), on the other hand, are undoubtedly of great benefit to the model performance. Overall, these results show that the chosen approach is powerful in modeling karst spring discharge, given that relevant and high-quality input data is present.

4.2 Lez Spring (France)

Figure 10 shows the modeling results for 2018 and 2019 at Lez spring in France with satisfying performance measure values (NSE, KGE = 0.77, $R^2 = 0.78$). The time series in general is characterized by distinct dry periods without any recharge due to anthropogenic water extraction in the saturated zone of the aquifer. These periods are quite accurately simulated, which was achieved by using a ReLU activation function that does not allow negative output values and that has been implemented for the output neuron instead of a classical linear activation. This makes learning zero output easier and agrees with the physical understanding that negative output is not possible. During optimization however, also a higher number of instabilities in terms of failed training attempts was observed. These failures were prone to a high sensitivity to the random number seed and could therefore be easily solved by choosing different seeds, nevertheless, careful training observation seems to be necessary when using ReLU activation output neurons. Further some inaccuracies in terms of underestimation of higher discharge events (e.g. 12/2018-01/2019) and overestimation of smaller events in the first half of the year 2019 are observed. The model uncertainty interval derived from Monte-Carlo dropout ensembles significantly higher compared to Aubach spring; however, a significantly higher dropout rate of 50% has been used. This on the one hand increases uncertainty, but on the other hand also makes training more robust and was chosen because no performance decrease compared to a lower dropout rate has been observed for Lez spring.

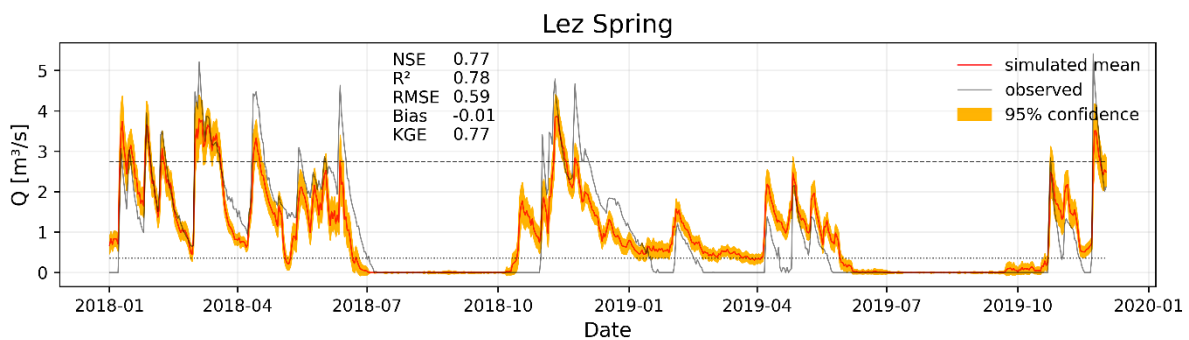


Figure 10: Modeling results for Lez spring in 2018 and 2019. Dashed and dotted lines: thresholds to determine low, medium and high flow.

Similarly as for Aubach spring, the model systematically underestimates high and medium flow, while low flow periods are overestimated on average (Table 6). However, low flow is not systematically too high, but rather unprecise for some events. Longer periods of zero discharge are captured well.

Table 6: Low, medium and high flow evaluation of the model performance at Lez spring.

	RMSE [m ³ /s]	Bias [m ³ /s]
Total	0.59	-0.01
High Flow	1.02	-0.78
Medium Flow	0.61	-0.14
Low Flow	0.43	0.23

4.3 Unica Springs (Slovenia)

Unica springs discharge time series represents the joint discharge of several springs feeding the Unica river. The CNN model can profit from a very long data basis of daily data (since 1961) during training and therefore shows high performance in terms of the error measures (NSE & $R^2 > 0.85$, KGE = 0.74), capturing the major dynamic of the spring quite accurately (Figure 11), despite climate input variables

were only available for two different climate stations, thus very few for such a large catchment (>800 km²). Further, the two climate stations (Postojna and Cerknica) represent different climate regimes and are separated by the karst massif in between, which is the major recharge area (Javorniki plateau) without any direct climate data available there. Overall, the model tends to underestimate high discharge events, but captures low flow periods nicely, with only slight overestimation of minor events. The time series repeatedly shows high discharge events with a plateau-like shape, which originates in a flooding of the polje, which makes it impossible to accurately monitor the true conditions. The CNN model simulates the high-discharge plateaus as separate peaks, which is false in terms of accuracy and in terms of what the model should have learned from the data, however, which also might have some conceptual truth underlying.

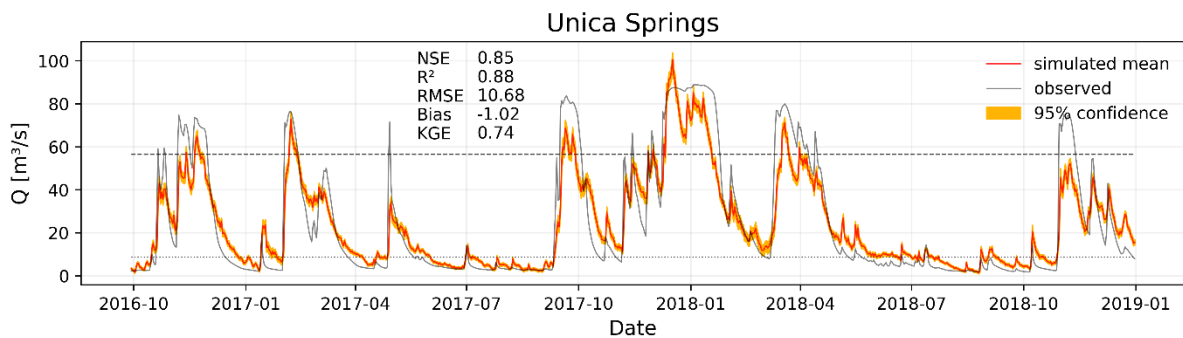


Figure 11: Modeling results for Unica springs mainly in 2017 and 2018. Dashed and dotted lines: thresholds to determine low, medium and high flow.

Regarding high, medium and low flow performance (Table 7), the largest part of the overall error clearly derives from high flow periods. In comparison with other test sites the high flow error has even more weight because of the already mentioned high flow plateaus. Further, in contrary to Aubach and Lez spring, not only low, but also medium flow is systematically overestimated. This could be the result of the attempt of the model to better fit the high flow periods during training, which maybe shifts the whole discharge curve slightly towards the upper limits.

Table 7: Low, medium and high flow evaluation of the model performance at Unica springs.

	RMSE [m ³ /s]	Bias [m ³ /s]
Total	10.68	-1.02
High Flow	20.23	-17.43
Medium Flow	9.43	1.62
Low Flow	4.25	3.39

4.4 Gato Cave Spring (Spain)

Similar to Unica springs, for Gato Cave spring a very long data basis of daily values is available for training. Probably related to this fact, the CNN model achieves high accuracy with NSE, R² and KGE values of 0.88 (Figure 12). The general dynamics of the discharge is nicely captured, and most peaks are neither over nor underestimated significantly. Nevertheless, single events (e.g. in the end of 2012 and 2014) are not very well captured, which, however, does not dominate the overall impression. The

model uncertainty derived from a 10% Monte Carlo dropout approach is low and it can be concluded that overall Gato Cave spring can be modeled accurately with the presented CNN approach.

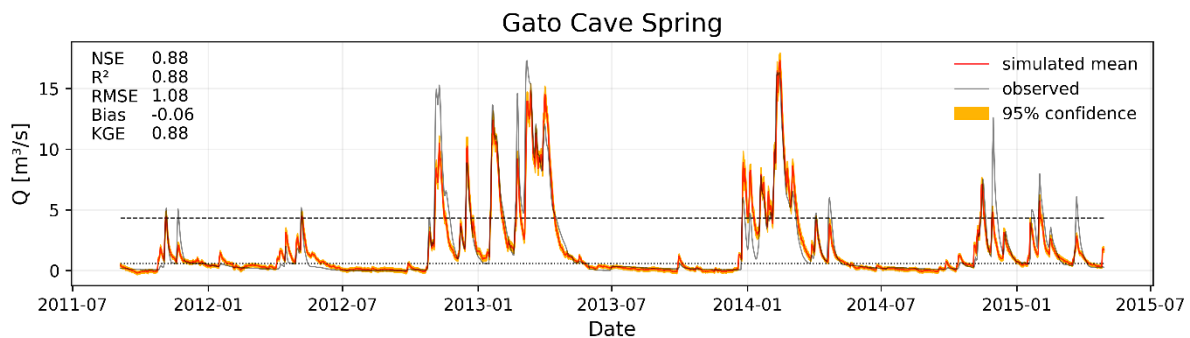


Figure 12: Modeling results for Gato cave spring in 2013 and 2014. Dashed and dotted lines: thresholds to determine low, medium and high flow.

Table 8 shows that especially low and medium flow performance of the ANN model at Gato Cave spring is highly satisfying. Similar to Unica springs results, these sections tend to be overestimated, but only very slightly, especially in comparison to the total variability. Again, the main errors derive from the high flow sections, which are harder to simulate, because they are generally underrepresented in the training data (which applies all other sites, too).

Table 8: Low, medium and high flow evaluation of the model performance at Gato Cave spring.

	RMSE [m ³ /s]	Bias [m ³ /s]
Total	1.08	-0.06
High Flow	2.43	-0.96
Medium Flow	0.99	0.06
Low Flow	0.31	0.10

4.5 Qachqouch Spring (Lebanon)

Qachqouch spring in Lebanon shows comparably poor data availability. The model has learned from only three years of daily data and the validation, optimization and testing periods are comparably short. Additionally, even when data is available, there is a significant amount of time without (relevant) discharge, thus where no input-output relation can be learned. This corresponds to the unsatisfying modeling results during the test period shown in Figure 13, with NSE, R² and KGE < 0.5, and no useful fit of the discharge events. Here the limitations of the CNN approach, which relies on a high amount of data to learn the system relationships, are clearly visible. Due to the characteristics of the discharge time series, it can be speculated that a significantly longer time series of daily values would be needed to successfully simulate Qachqouch spring. Furthermore, it is unlikely that the model would significantly profit from feeding in hourly data, because the dynamics of the spring is rather low. Maybe a rather moderate increase of the sampling interval to 12h or 8h could be useful to increase the number of available samples. Due to the unsatisfying performance no detailed analysis for high, medium and low flow periods at Qachqouch spring was performed.

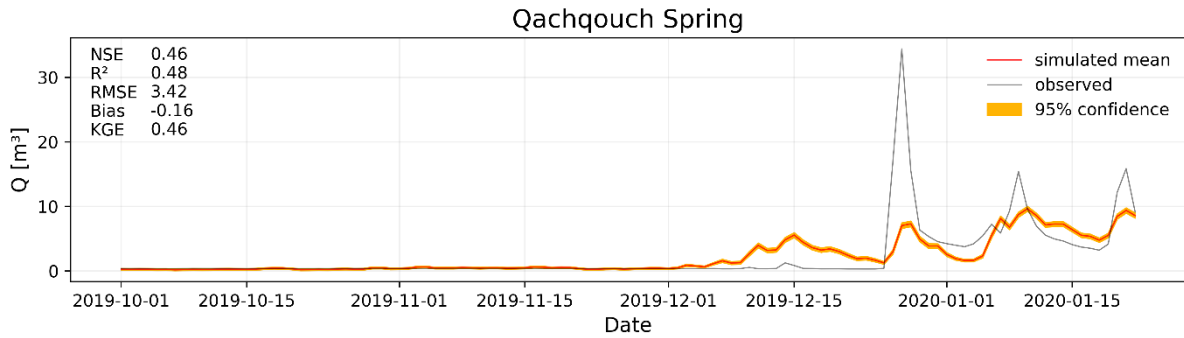


Figure 13: Modeling results for Qachqouch spring in the end of 2019 and the beginning of 2020.

4.6 Nymphaea Spring (Tunisia)

4.6.1 MLP

After 250 iterations for the daily data and 152 iterations for the weekly data using Bayesian optimization, we obtained the following hyperparameters.

Table 9: Optimal hyperparameters of the MLP model

Hyperparameter	MLP for daily data	MLP for weekly data
Sequence length	174 days	27 weeks (189 days)
Batch size	115	57
Learning rate	0.01	0.1
Dense size 1	164	237
Dense size 2	185	108
Dropout	0.07	0

The calibration phase for our MLP model is good. However, the weekly data provide good results ($R^2=0.84$; $NSE=0.84$) compared to the daily data ($R^2=0.75$; $NSE=0.77$). For the test set we obtained the following result (Figure 14 and Figure 15):

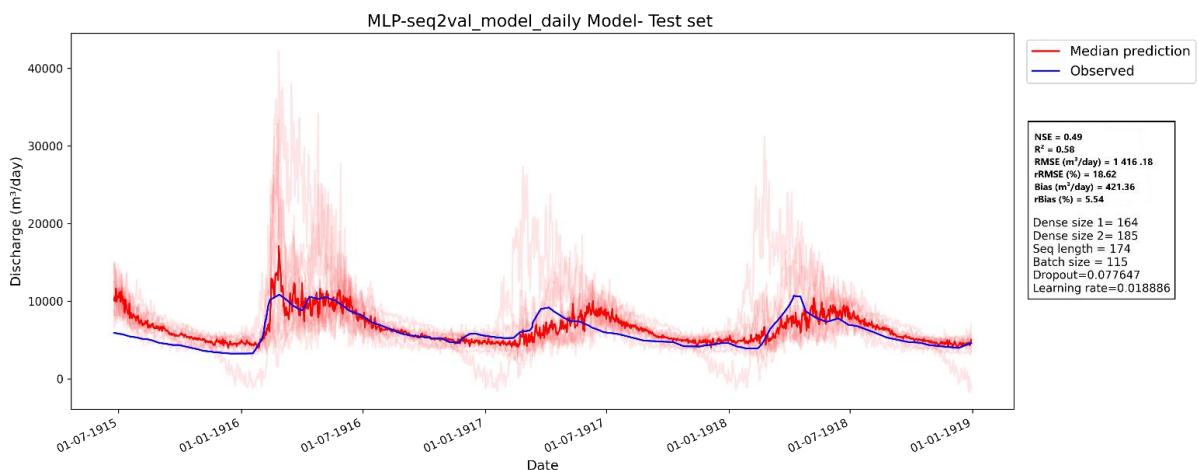


Figure 14: MLP seq2val test set result on daily data

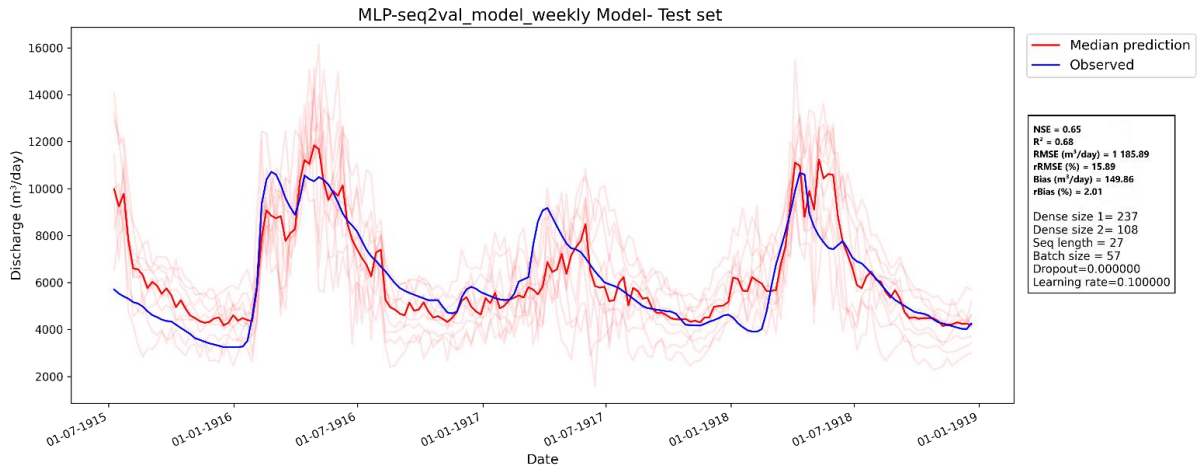


Figure 15: MLP seq2val test set result on weekly data.

4.6.2 CNN

After 200 iterations for the daily data and 200 iterations for the weekly data using Bayesian optimization, we obtained the following hyperparameters (Table 10).

Table 10: Optimal hyperparameters of the CNN model

Hyperparameter	CNN for daily data	CNN for weekly data
Sequence length	182	24 weeks= 168 days
Batch size	155	209
Learning rate	0.04	0.1
Filters	167	156
Dense size	136	150
Dropout	0.15	0

The calibration phase for the CNN model is also good. The weekly data provide good results ($R^2=0.84$; $NSE=0.85$) compared to the daily data ($R^2=0.85$ $NSE=0.85$). These results are better than those of the MLP model. For our test set, we obtain the following results (Figure 16 and Figure 17).

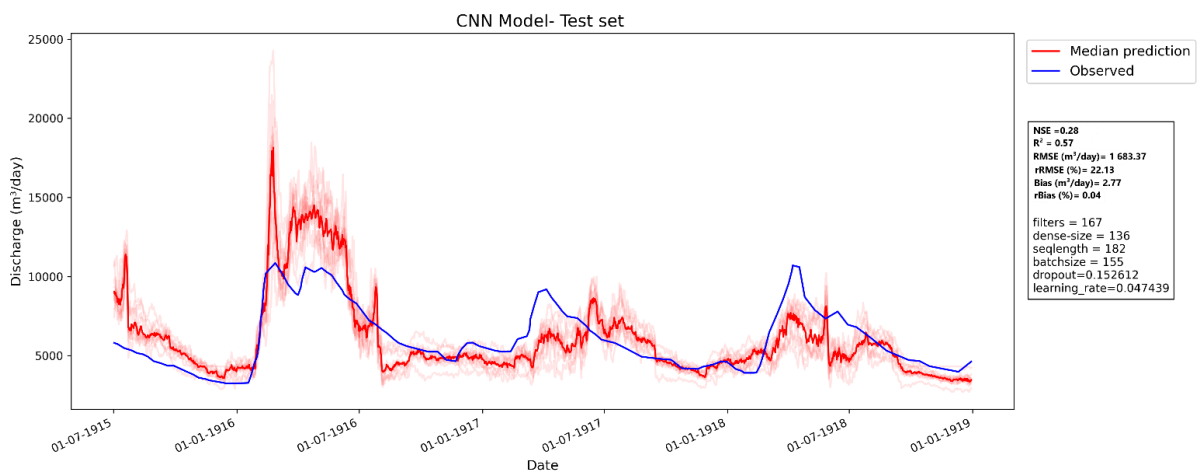


Figure 16: CNN seq2val test set result on daily data

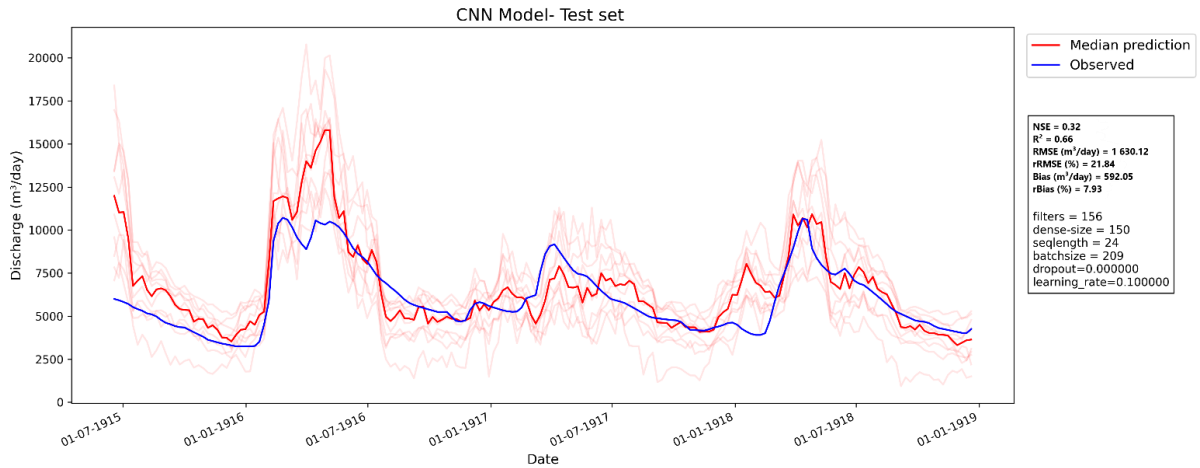


Figure 17: CNN seq2val test set result on weekly data.

4.6.3 LSTM

For the daily data, after 51 iterations that lasted about 30 hours and without significant performance improvement, we did not obtain an optimal result. As for the weekly data, after 215 iterations through Bayesian optimization, we obtained the following hyperparameters (Table 11):

Table 11: Optimal hyperparameters of the LSTM model

Hyperparameter	LSTM for weekly data
Sequence length	40 weeks= 280 days
Batch size	2
Learning rate	0.04

The calibration phase for our LSTM model is good. Expected to provide good results with time series like flow, the results obtained are acceptable with $R^2=0.72$ and $NSE=0.75$. These results are average compared to the CNN model and the MLP model. For the test set (Figure 18) below, the performances are average ($R^2=0.17$; $NSE=0.72$):

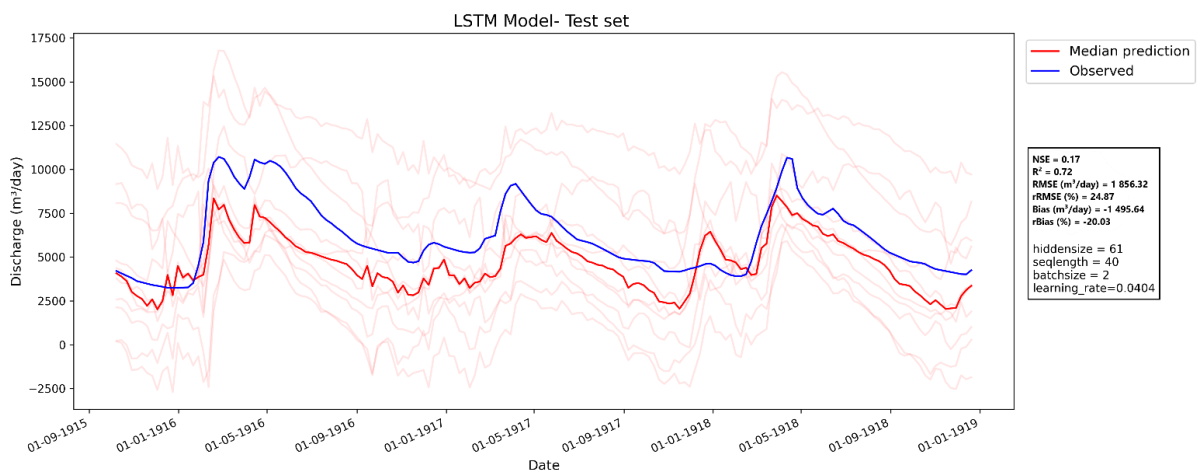


Figure 18: LSTM seq2val test set result on weekly data.

For all our models considered at Zaghouan site, the simulations performed on weekly data provided better results than the simulations on daily data, we deduce that the weekly scale is the most relevant in the hydrodynamic study of the Zaghouan karst. This is due to the fact that (i) the daily discharge

were obtained by interpolation of the weekly discharge, (ii) the cumulative uncertainties of the discharge measurements and (iii) the cumulative uncertainties of the daily rainfall measurements, some of which were taken every 3 days. Furthermore, the MLP model gave the best results on the weekly test set ($R^2=0.65$; $NSE=0.68$) compared to the CNN ($R^2= 0.32$; $NSE=0.66$) and LSTM ($R^2=0.17$; $NSE=0.72$) models. LSTM gave the worst results. The distribution of predicted weekly discharge in relation to observed weekly discharge shows an overestimation in our forecasting.

Notwithstanding the use of a synthetic temperature and pressure series, our results are on the whole acceptable. Once the real data are obtained, we will be able to better understand and interpret the influence of temperature and pressure on the functioning of the karst. The sequence length of the MLP and CNN models on the weekly data are of the same order (CNN: 24; MLP: 27), i.e. about 6 months. It is therefore necessary to know the climatic data (rain, temperature and pressure) on the karst for the previous 6 months for a better forecasting of the discharge at 6 months (+) 1 day. Moreover, an auto-analysis of the data we have carried out has provided a significant correlation for a lag of 126 days, i.e. about 4 months, between rainfall and discharge. Therefore, the lag-time would be between 4 months (by analysis of observations) and 6 months (by modelling), for our karst system.

4.7 Comparison with lumped parameter model results

A direct comparison with the results of the lumped parameter modeling (LPM) (Deliverable 4.2) is difficult. Both approaches are fundamentally different and also show very different requirements e.g. in terms of available data. ANNs possibly profit from every additional input time period and parameter, but also require a certain amount of data to be able to learn the respective relationships between climate and spring discharge. On the one hand, this enables ANNs to learn directly from the data without specific system knowledge priorly necessary, on the other hand no additional system knowledge can be derived from the results, in contrary to the lumped parameter approach. Therefore, the input data used for both approaches is different and varies site specifically. For ANNs mostly all directly available climate parameters were used as inputs, for the lumped parameter approach a uniform set of inputs including e.g. redistributed precipitation and computed evapotranspiration time series were used for all sites. Because of different input data, the test periods of both approaches are not identical for Lez spring, and slightly different for Gato Cave spring (identically for all other sites). This should be kept in mind when comparing performance criteria of both approaches. Nevertheless, for a rough comparison several performance measures of both models for several test sites are compiled in Table 12.

Table 12: Comparison of lumped parameter modeling (LPM) and ANN results. Since both models use different input data and the test periods for Lez spring and Gato Cave spring do not match (only slightly different for Gato Cave spring), results should be interpreted with care.

Site	Approach	NSE []	KEGE []	R^2 []	RMSE [m^3/s]	Bias [m^3/s]
Aubach	LPM	0.42	0.69	0.49	0.92	0.08
	ANN	0.82	0.90	0.83	0.51	-0.06
Lez	LPM	0.70	0.65	0.76	0.68	0.31
	ANN	0.77	0.77	0.78	0.59	-0.01
Unica	LPM	0.82	0.70	0.88	11.55	3.62
	ANN	0.85	0.74	0.88	10.68	-1.02
Gato Cave	LPM	0.90	0.79	0.92	1.00	0.25
	ANN	0.88	0.88	0.88	1.08	-0.06
Quachqouch	LPM	0.89	0.90	0.89	1.54	-0.02
	ANN	0.46	0.46	0.48	3.42	-0.16

The results of the ANN based modeling are mostly better than for the LPM approach. Especially for modeling the complex Aubach spring system, ANNs clearly outperform the LPM model. Similarly, ANNs show better results at Lez spring, however the test periods do not match here, which makes a comparison difficult. No clear differences can be found at Unica springs and Gato Cave spring, where partly ANN and partly LPM show better performance. Unica spring is directly comparable, but also at Gato Cave spring the test period is almost identical. The Qachqouch results demonstrate the advantages of LPMs that need less data (in terms of length of the data period) to successfully model a karst spring system. While ANNs fail here, the LPM shows rather good results.

5 Conclusions

The results show that the 1D-CNN approach can be easily implemented to successfully and accurately model karst spring discharge under different climatic conditions, as long as a sufficient amount of historical data (discharge, climatic inputs) is available to train the model. It is possible to model systems showing significant different properties such as catchment size, complexity and hydraulic properties. Four out of five springs were modeled with good to very high accuracy, only for Qachqouch spring the approach was not successful, most certainly because of insufficient data availability for both climatic inputs and spring discharge. The chosen approach is adaptable to specific data properties as the example of Lez spring show. Here the modeler can easily teach that negative discharge values are forbidden and hence can increase physical meaning of the modeling. This is in principle true for all spring discharge time series, as negative discharge is not possible, however as long as the (close-to-) zero discharge is natural (which is not the case for Lez spring), the model usually learns this relation by itself reliably. It can be concluded that for a mere simulation purpose, the CNN approach is associated with comparably low effort and a legitimate alternative to conventional model approaches such as lumped parameter modeling. At Zaghouan site the CNN approach was outperformed by a MLP model (on weekly timescale), which, however, showed strong dependency on the random seed initialization. Here, the CNN again showed that it is more stable than other approaches.

References

- Abadi, M., Agarwal, A., Barham, P., Brevdo, E., Chen, Z., Citro, C., Corrado, G.S., Davis, A., Dean, J., Devin, M., Ghemawat, S., Goodfellow, I., Harp, A., Irving, G., Isard, M., Jia, Y., Jozefowicz, R., Kaiser, L., Kudlur, M., Levenberg, J., Mane, D., Monga, R., Moore, S., Murray, D., Olah, C., Schuster, M., Shlens, J., Steiner, B., Sutskever, I., Talwar, K., Tucker, P., Vanhoucke, V., Vasudevan, V., Viegas, F., Vinyals, O., Warden, P., Wattenberg, M., Wicke, M., Yu, Y., Zheng, X., 2015. TensorFlow: Large-Scale Machine Learning on Heterogeneous Distributed Systems 19.
- Bergström, S., 1995. The HBV model, in: Singh, V.P. (Ed.), *Computer Models of Watershed Hydrology*. Water Resources Publications, Colorado, USA, pp. 443–476.
- Bergström, S., 1975. The development of a snow routine for the HBV-2 model. *Hydrol. Res.* 6, 73–92. <https://doi.org/10/gkqz5>
- Chen, Z., Auler, A.S., Bakalowicz, M., Drew, D., Griger, F., Hartmann, J., Jiang, G., Moosdorf, N., Richts, A., Stevanovic, Z., Veni, G., Goldscheider, N., 2017a. The World Karst Aquifer Mapping project: concept, mapping procedure and map of Europe. *Hydrogeol. J.* 25, 771–785. <https://doi.org/10/f98h6g>
- Chen, Z., Hartmann, A., Goldscheider, N., 2017b. A new approach to evaluate spatiotemporal dynamics of controlling parameters in distributed environmental models. *Environ. Model. Softw.* 87, 1–16. <https://doi.org/10.1016/j.envsoft.2016.10.005>
- Chen, Z., Hartmann, A., Wagener, T., Goldscheider, N., 2018. Dynamics of water fluxes and storages in an Alpine karst catchment under current and potential future climate conditions. *Hydrol Earth Syst Sci* 17. <https://doi.org/10.5194/hess-22-3807-2018>
- Chollet, F., 2015. Keras.
- Faydi, T., 2021. La modélisation hydrodynamique des aquifères karstiques de Djebel Zaghouan par karstmod. *Mastère de Recherche spécialité : Modélisation en Hydraulique et Environnement*. ENIT, Tunis.
- Gupta, H.V., Kling, H., Yilmaz, K.K., Martinez, G.F., 2009. Decomposition of the mean squared error and NSE performance criteria: Implications for improving hydrological modelling. *J. Hydrol.* 377, 80–91. <https://doi.org/10.1016/j.jhydrol.2009.08.003>
- Hock, R., 1999. A distributed temperature-index ice- and snowmelt model including potential direct solar radiation. *J. Glaciol.* 45, 101–111. <https://doi.org/10/ggnvkt>

- Hunter, J.D., 2007. Matplotlib: A 2D Graphics Environment. *Comput. Sci. Eng.* 9, 90–95. <https://doi.org/10.1109/mcse.2007.55>
- Jeannin, P.-Y., Artigue, G., Butscher, C., Chang, Y., Charlier, J.-B., Duran, L., Gill, L., Hartmann, A., Johannet, A., Jourde, H., Kavousi, A., Liesch, T., Liu, Y., Lüthi, M., Malard, A., Mazzilli, N., Pardo-Igúzquiza, E., Thiéry, D., Reimann, T., Schuler, P., Wöhling, T., Wunsch, A., 2021. Karst modelling challenge 1: Results of hydrological modelling. *J. Hydrol.* 600, 126508. <https://doi.org/10.1016/j.jhydrol.2021.126508>
- Johannet, A., Mangin, A., D'Hulst, D., 1994. Subterranean water infiltration modelling by neural networks: use of water source flow, in: *ICANN '94: Proceedings of the International Conference on Artificial Neural Networks Sorrento, Italy, 26–29 May 1994 Volume 1, Parts 1 and 2. Presented at the International Conference on Artificial Neural Networks, Springer Berlin Heidelberg, Sorrento, Italy*, pp. 1033–1036.
- Kollat, J.B., Reed, P.M., Wagener, T., 2012. When are multiobjective calibration trade-offs in hydrologic models meaningful? *Water Resour. Res.* 48. <https://doi.org/10/gkq5k>
- Kong-A-Siou, L., Johannet, A., Borrell Estupina, V., Pistre, S., 2015. Neural networks for karst groundwater management: case of the Lez spring (Southern France). *Environ. Earth Sci.* 74, 7617–7632. <https://doi.org/10.1007/s12665-015-4708-9>
- Lebigot, E.O., 2010. Uncertainties: a Python package for calculations with uncertainties.
- LeCun, Y., Bengio, Y., Hinton, G., 2015. Deep learning. *Nature* 521, 436–444. <https://doi.org/10.1038/nature14539>
- Mbah, T.J., Ye, H., Zhang, J., Long, M., 2021. Using LSTM and ARIMA to Simulate and Predict Limestone Price Variations. *Min. Metall. Explor.* 38, 913–926. <https://doi.org/10/gmhg5w>
- McKinney, W., 2010. Data Structures for Statistical Computing in Python. Presented at the Python in Science Conference, Austin, Texas, pp. 56–61. <https://doi.org/10.25080/majora-92bf1922-00a>
- Nash, J.E., Sutcliffe, J.V., 1970. River flow forecasting through conceptual models part I—A discussion of principles. *J. Hydrol.* 10, 282–290. [https://doi.org/10.1016/0022-1694\(70\)90255-6](https://doi.org/10.1016/0022-1694(70)90255-6)
- Nogueira, F., 2014. Bayesian Optimization: Open source constrained global optimization tool for Python.
- Pedregosa, F., Varoquaux, G., Gramfort, A., Michel, V., Thirion, B., Grisel, O., Blondel, M., Prettenhofer, P., Weiss, R., Dubourg, V., Vanderplas, J., Passos, A., Cournapeau, D., 2011. Scikit-learn: Machine Learning in Python. *J. Mach. Learn. Res.* 12, 2825–2830.
- Reback, J., McKinney, W., Jbrockmendel, Bossche, J.V.D., Augspurger, T., Cloud, P., Gfyoung, Sinhrks, Klein, A., Roeschke, M., Hawkins, S., Tratner, J., She, C., Ayd, W., Terji Petersen, Garcia, M., Schendel, J., Hayden, A., MomIsBestFriend, Jancauskas, V., Battiston, P., Skipper Seabold, Chris-B1, H-Vetinari, Hoyer, S., Overmeire, W., Alimcmaster1, Kaiqi Dong, Whelan, C., Mortada Mehayar, 2020. pandas-dev/pandas: Pandas 1.0.3. Zenodo. <https://doi.org/10.5281/ZENODO.3509134>
- Sagna, J., 2000. Study and modeling of Zaghouan karst sources, Master thesis. ENIT.
- Seibert, J., 2000. Multi-criteria calibration of a conceptual runoff model using a genetic algorithm. *Hydrol. Earth Syst. Sci.* 4, 215–224. <https://doi.org/10/crmzd7>
- Shanker, M., Hu, M.Y., Hung, M.S., 1996. Effect of data standardization on neural network training. *Omega* 24, 385–397. <https://doi.org/10/ck4tv5>
- van der Walt, S., Colbert, S.C., Varoquaux, G., 2011. The NumPy Array: A Structure for Efficient Numerical Computation. *Comput. Sci. Eng.* 13, 22–30. <https://doi.org/10.1109/mcse.2011.37>
- van Rossum, G., 1995. Python tutorial.
- Wunsch, A., Liesch, T., Broda, S., 2021. Groundwater level forecasting with artificial neural networks: a comparison of long short-term memory (LSTM), convolutional neural networks (CNNs), and non-linear autoregressive networks with exogenous input (NARX). *Hydrol. Earth Syst. Sci.* 25, 1671–1687. <https://doi.org/10.5194/hess-25-1671-2021>